

# Free Vibrations of Functionally Graded Circular Cylindrical Shells under Internal Pressure

## A. Davar

Department of Mechanical Engineering,  
Islamic Azad University, Damavand Branch, Damavand, Iran  
E-mail: [davar78@gmail.com](mailto:davar78@gmail.com)

## S. M. R. Khalili

Department of Mechanical Engineering,  
K.N. Toosi University of Technology, Tehran, Iran  
Faculty of Engineering, Kingston University, London, UK  
E-mail: [smrkhalili2005@gmail.com](mailto:smrkhalili2005@gmail.com)

## H. Hadavinia

School of Mechanical & Automotive Engineering,  
Kingston University, London, UK  
E-mail: [h.hadavinia@kingston.ac.uk](mailto:h.hadavinia@kingston.ac.uk)  
\*Corresponding author

Received: 14 Mars 2012, Revised: 25 April 2012, Accepted: 9 June 2012

**Abstract:** Free vibration of simply supported circular cylindrical shell made of Functionally Graded Material (FGM) under internal pressure was investigated. The effective material properties are assumed to vary continuously along the thickness direction according to a volume fraction power law distribution. First order shear deformation theory based on Love's first approximation theory was utilized in the equilibrium equations. The effects of FGM parameters such as material configuration and power law exponent, internal pressure as well as geometrical parameters such as thickness to radius and length to radius ratios on the vibration behavior were investigated. The validation of the results was achieved by comparing with those available in the literature. The results show that the vibration characteristics of Functionally Graded (FG) shells are greatly influenced by FGM parameters. Moreover, internal pressure and geometrical parameters considerably influence the frequency behavior regarded to different values of FGM parameters.

**Keywords:** Cylindrical Shell, Functionally Graded Material, Free Vibration, Internal Pressure

**Reference:** A. Davar, S. M. R. Khalili and H. Hadavinia, "Free Vibrations of Functionally Graded Circular Cylindrical Shells under Internal Pressure", Int J of Advanced Design and Manufacturing Technology, Vol. 6/ No. 4, 2013, pp. 47-56.

**Biographical notes:** **A. Davar** received his PhD in Mechanical Engineering at the K.N. Toosi University of Technology. He is currently an invited lecturer at the Department of Mechanical Engineering, Azad University, Damavand Branch. **S. M. R. Khalili** received his PhD in Applied Mechanics from Indian Institute of Technology (I.I.T), New Delhi, India in 1992. He is currently a Professor at the Department of Mechanical Engineering, K.N.Toosi University of Technology, Tehran, Iran, and also Visiting Professor at Faculty of Engineering, University of Kingston, London, UK. **H. Hadavinia** is an Associate Professor of Engineering Faculty at the Kingston University, London, UK. His main work is concerned with measuring, modelling and predicting the performance and behaviour of composite structures, experimental and numerical modelling of adhesives and bonded joints, fatigue testing and modelling of bonded structures and lifetime prediction methodology of bonded composites and metallic materials.

---

## 1 INTRODUCTION

---

The advantage of using functionally graded materials (FGMs) is that they are able to withstand high temperature-gradient environments while maintaining their structural integrity. FG shells as primary structural component material in advanced industries have been a subject of considerable interest and concern in recent years. Loy et al. studied the influence of volume fractions and configurations of the constituent materials on the natural frequencies of FG cylindrical shells [1]. Their analysis was carried out with strain-displacement relations from Love's shell theory and the eigenvalue governing equation is obtained using Rayleigh-Ritz method.

It was pointed out that FG shell frequency behavior is similar to homogenous shells. Pradhan et al. studied the effects of boundary conditions and volume fractions on the natural frequencies of the FG cylindrical shell using Rayleigh method [2]. Their analysis was achieved similar to Ref., the only difference is that they used modal beam function instead of trigonometric function used by Loy et al. in axial direction [1]. They showed that boundary conditions have considerable effect on the frequencies of the FG shell. Ng et al. presented the dynamic stability analysis of FG cylindrical shell under periodic axial loading [3]. A system of Mathieu-Hill equations was obtained using a normal-mode expansion of the equations of motion. It was also found that reasonable control can be achieved on the natural frequencies and dynamic instability regions by correctly varying the material composition.

Liew et al. investigated the linear and nonlinear vibration of a coating-FGM-substrate cylindrical panel with general boundary conditions subjected to a temperature field [4]. The theoretical formulation was based on geometric nonlinearity in von-Karman sense and the first order shear deformation theory. Numerical results were presented for three-layer cylindrical panels which consist of an aluminum substrate and a zirconia coating with an aluminum-zirconia graded layer sandwiched in between. It was shown that both the linear and nonlinear vibration behavior of the cylindrical panel are greatly influenced by vibration amplitude, out-of-plane boundary conditions, and geometric parameters. Darabi et al. presented a simple solution of the dynamic stability of FG shells under periodic axial loading based on large deflection theory [5].

The equations of motion were solved by Galerkin procedure. Bolotin's method was then employed to obtain the steady-state vibrations for non-linear Mathieu equations. It was confirmed that the characteristics of large deflection were significantly influenced by volume fraction distribution,

circumferential wave number and shell aspect ratio. It was found that reasonable control could be achieved on the steady-state vibrations amplitudes by correctly varying the power law exponent of volume fractions. Ansari and Darvizeh presented general analytical approaches to investigate the effect of boundary conditions on the free vibration behavior of FG shells [6].

Theoretical formulation was developed based on first order shear deformation theory. The modal forms were assumed to have the axial dependency in the form of Fourier series whose derivatives were legitimized using Stoke's transformation. They compared the results with those reported by and good agreement was observed [2]. It was cleared that alteration of the natural frequency of a FGM shell is easily viable by varying the volume fraction of its constituent materials. Haddadpour et al. applied the Galerkin method to investigate free vibration analysis of FG cylindrical shells including thermal effects [7]. The equations of motion are based on Love's shell theory.

The natural frequencies of FG cylindrical shells were determined in four sets of in-plane boundary conditions. They compared the natural frequencies with those reported by [1] and close agreement was observed. Their results show that while the critical mode numbers remain unchanged, increasing the power law index for all boundary conditions influences natural frequencies. Khalili et al. studied the forced vibrations of FG cylindrical shell using first order shear deformation theory [8]. They studied the effect of power law exponent on the transient response of strains as well as displacements of the shell under locally applied lateral impulse load and showed this effect is considerable.

None of the preceding studies, however, dealt with the effect of internal pressure on the free vibrations of FG thin shells. Therefore, a comprehensive study and understanding of free vibrations of initially stressed FG thin shells is essential. The present work addresses an analytic solution to the free vibration problem of FG cylindrical shell under internal pressure.

---

## 2 DEFINITION OF MATERIAL PROPERTIES FOR FG SHELLS

---

The volume fraction of the constituent materials is considered to vary continuously along the shell thickness. The material properties  $P$  can be expressed as a function of temperature as [1]:

$$P = P_0(P_{-1}T^{-1} + 1 + P_1T + P_2T^2 + P_3T^3) \quad (1)$$

Where  $P_0, P_{-1}, P_1, P_2$  and  $P_3$  are the coefficients of temperature  $T$  ( $^{\circ}\text{K}$ ) expressed in Kelvin and are unique to the constituent materials. For a cylindrical shell with a uniform thickness  $h$  and a reference surface at its mid surface with the thickness direction coordinate  $z$ , the volume fraction of each constituent material can be written as:

$$V_f = \left(\frac{z + h/2}{h}\right)^N \quad (2)$$

Where  $N$  is the power law exponent,  $0 \leq N \leq \infty$ . For a FG material with two constituent materials, the Young's modulus  $E$ , Poisson's ratio  $\nu$  and mass density  $\rho$  can be expressed as:

$$\begin{aligned} E &= (E_1 - E_2) \left(\frac{2z + h}{2h}\right)^N + E_2 \\ \nu &= (\nu_1 - \nu_2) \left(\frac{2z + h}{2h}\right)^N + \nu_2 \\ \rho &= (\rho_1 - \rho_2) \left(\frac{2z + h}{2h}\right)^N + \rho_2 \end{aligned} \quad (3)$$

### 3 GOVERNING EQUATIONS

A circular cylindrical shell with mean radius of  $R$ , thickness  $h$  and length  $L$  is shown in Fig. 1.

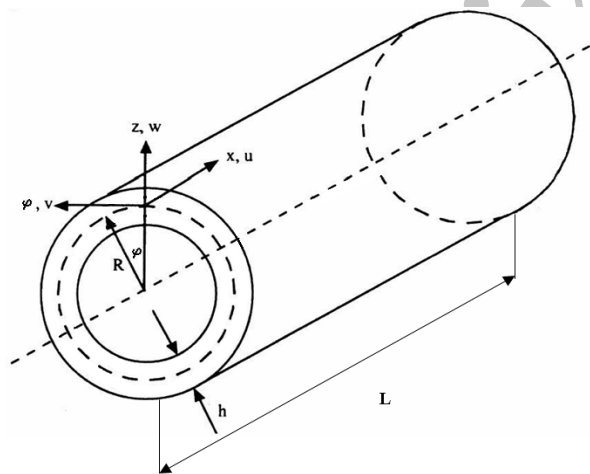


Fig. 1 Geometry of cylindrical shell and referenced coordinate system

The origin of the orthogonal coordinate system  $(x, \phi, z)$  is placed at the mid surface at the end of the cylinder. The displacements of the cylinder in the  $x, \phi$  and  $z$  directions are defined by  $u, v$  and  $w$ , respectively. The deformations of the shell are assumed to be small. Based on First order Shear Deformation Theory (FSDT), the equilibrium equations for a cylindrical shell are as follows [9]:

$$N_{x,x} + N_{x\phi,\phi}/R + P(u_{,\phi\phi}/R + w_{,x}) = I_1 u_{,tt} + I_2 \beta_{x,tt} \quad (6)$$

$$\begin{aligned} N_{x\phi,x} + N_{\phi,\phi}/R + Q_{\phi}/R + P(v_{,\phi\phi}/R + w_{,\phi}) = \\ (I_1 + 2I_2/R)v_{,tt} + (I_2 + I_3/R)\beta_{\phi,tt} \end{aligned} \quad (7)$$

$$\begin{aligned} Q_{x,x} + Q_{\phi,\phi}/R - N_{\phi}/R \\ - P(u_{,x} - v_{,\phi}/R - w_{,\phi\phi}/R) = I_1 w_{,tt} \end{aligned} \quad (8)$$

$$M_{x,x} + M_{x\phi,\phi}/R - Q_x = I_3 \beta_{x,tt} + I_2 u_{,tt} \quad (9)$$

$$M_{x\phi,x} + M_{\phi,\phi}/R - Q_{\phi} = I_3 \beta_{\phi,tt} + (I_2 + I_3/R)v_{,tt} \quad (10)$$

Where ‘,’ denotes differentiation with respect to time or coordinate. In the above equations,  $\beta_x$  and  $\beta_{\phi}$  are the slopes in the plane of  $x-z$  and  $\phi-z$ , respectively.  $P$  is internal pressure. The terms  $I_1, I_2$  and  $I_3$  are defined as:

$$(I_1, I_2, I_3) = \int_{-h/2}^{h/2} (1, z, z^2) \rho dz \quad (11)$$

In Eqs. (6) to (10), the stress resultants  $N^T = \{N_x, N_{\phi}, N_{x\phi}\}$ , moments  $M^T = \{M_x, M_{\phi}, M_{x\phi}\}$ , and transverse shear forces  $(Q_x, Q_{\phi})$  are defined as:

$$\begin{Bmatrix} N \\ M \end{Bmatrix} = \begin{bmatrix} A & B \\ B & D \end{bmatrix} \begin{Bmatrix} e \\ \kappa \end{Bmatrix}, \quad Q = [A] \begin{Bmatrix} \gamma_{xz}^{\circ} \\ \gamma_{\phi z}^{\circ} \end{Bmatrix} \quad (12)$$

Where the extensional stiffnesses  $A_{ij}$  ( $i, j = 1, 2, 6$ ), coupling stiffnesses  $B_{ij}$  ( $i, j = 1, 2, 6$ ), bending stiffnesses  $D_{ij}$  ( $i, j = 1, 2, 6$ ) and transverse shear stiffnesses  $A_{ij}$  ( $i, j = 4, 5$ ) are:

$$(A_{ij}, B_{ij}, D_{ij}) = \int_{-h/2}^{h/2} Q_{ij}(1, z, z^2) dz \quad (i, j = 1, 2, 6) \quad (13)$$

$$A_{ij} = k_0 \int_{-h/2}^{h/2} Q_{ij} dz \quad (i, j = 4, 5)$$

$$Q_{11} = Q_{22} = \frac{E}{1-\nu^2}, \quad Q_{12} = \frac{\nu E}{1-\nu^2}$$

$$Q_{44} = Q_{55} = Q_{66} = \frac{E}{2(1+\nu)} \quad (14)$$

$$Q_{16} = Q_{26} = Q_{45} = 0$$

Where  $k_0$  in Eq. (13) is the shear correction factor introduced by Mindlin and is equal to  $\pi^2/12$  [9]. In Eq. (12),  $e^T = \{\epsilon_x^{\circ}, \epsilon_{\phi}^{\circ}, \gamma_{x\phi}^{\circ}\}$  and  $\kappa^T = \{\kappa_x, \kappa_{\phi}, \kappa_{x\phi}\}$  are strain

and curvature vectors of the mid surface, which are both related to the displacements of the cylindrical shell by Love's first approximation theory as defined in Ref. [9]:

$$\begin{cases} \{\varepsilon_x^\circ, \varepsilon_\varphi^\circ, \gamma_{x\varphi}^\circ\} = \{u_{,x}, v_{,\varphi}/R + w/R, u_{,\varphi}/R + v_{,x}\} \\ \{\kappa_x, \kappa_\varphi, \kappa_{x\varphi}\} = \{\beta_{x,x}, \beta_{\varphi,\varphi}/R, \beta_{x,\varphi}/R + \beta_{\varphi,x}\} \\ \{\gamma_{xz}^\circ, \gamma_{\varphi z}^\circ\} = \{\beta_x + w_{,x}, \beta_\varphi + w_{,\varphi}/R - v/R\} \end{cases} \quad (15)$$

The boundary conditions for the cylindrical shell which is simply supported along its curved edges at  $x = 0$  and  $x = L$  are considered as:

$$v = w = N_x = M_x = \beta_\varphi = 0 \quad (16)$$

In order to satisfy the boundary conditions,  $u, v, w, \beta_x$  and  $\beta_\varphi$  are defined by double Fourier series as:

$$\begin{aligned} u(x, \varphi, t) &= A_{mn} \cos \frac{m\pi x}{L} \cos n\varphi e^{i\omega_{mn}t} \\ v(x, \varphi, t) &= B_{mn} \sin \frac{m\pi x}{L} \sin n\varphi e^{i\omega_{mn}t} \\ w(x, \varphi, t) &= C_{mn} \sin \frac{m\pi x}{L} \cos n\varphi e^{i\omega_{mn}t} \\ \beta_x(x, \varphi, t) &= D_{mn} \cos \frac{m\pi x}{L} \cos n\varphi e^{i\omega_{mn}t} \\ \beta_\varphi(x, \varphi, t) &= E_{mn} \sin \frac{m\pi x}{L} \sin n\varphi e^{i\omega_{mn}t} \end{aligned} \quad (17)$$

In Eqs. (17),  $\omega_{mn}$  (rad/sec) are the natural angular frequencies related to mode number ( $m, n$ ) where  $m$  is the axial half wave number and  $n$  is the circumferential wave number. Also,  $A_{mn}, B_{mn}, C_{mn}, D_{mn}$  and  $E_{mn}$  are the constant amplitudes of vibrations regarded to the natural mode shapes and are calculated using the property of the orthogonality of mode shape with respect to mass matrix.

#### 4 FREE VIBRATIONS ANALYSIS

In order to solve the free vibration problem, first the displacement components, Eqs. (17), are put into the strain and curvature relations, Eqs. (15), and the result into the stress resultants, Eq. (12). Then the stress resultants, Eq. (12), are substituted in the governing equations of motion, Eqs. (6) to (10). After performing the mentioned substitutions, the governing equations could be simplified in the following form:

$$[L]\{U\} = \{0\} \quad (18)$$

Where

$$L = \begin{bmatrix} L_{11} & L_{12} & L_{13} & L_{14} & L_{15} \\ L_{21} & L_{22} & L_{23} & L_{24} & L_{25} \\ L_{31} & L_{32} & L_{33} & L_{34} & L_{35} \\ L_{41} & L_{42} & L_{43} & L_{44} & L_{45} \\ L_{51} & L_{52} & L_{53} & L_{54} & L_{55} \end{bmatrix}, U = \begin{Bmatrix} u \\ v \\ w \\ \beta_x \\ \beta_\varphi \end{Bmatrix} \quad (19)$$

$L_{ij}$  are the differential operators and are shown in Appendix. Eq. (18) is an eigen value problem in which the eigen values are the natural frequencies,  $\omega_{mn}$ , and the corresponding eigen vectors are named the mode shapes. Eq. (18) could be rewritten in the following form:

$$[K_{ij}] - \omega_{mn}^2 [M_{ij}] \{A_{mn} B_{mn} C_{mn} D_{mn} E_{mn}\}^T = \{0\} \quad (21)$$

(i, j = 1, ..., 5)

Where  $K_{ij}$  and  $M_{ij}$  are stiffness and mass matrices, respectively. By setting determinant of coefficients in Eq. (20) equal to zero, the characteristic frequency equation is derived as:

$$\delta_1 \omega^{10} + \delta_2 \omega^8 + \delta_3 \omega^6 + \delta_4 \omega^4 + \delta_5 \omega^2 + \delta_6 = 0 \quad (21)$$

Where  $\delta_i$  are constant coefficients. By solving equation (21), the natural frequencies,  $\omega_{mn}$ , are calculated. By substituting these natural frequencies back into Eq. (20), constant amplitudes of free vibrations regarded to the natural mode number ( $m, n$ ) are obtained. The smallest natural frequency is called fundamental frequency,  $\omega_f$ .

#### 5 RESULTS AND DISCUSSION

The material properties are listed in Table 1. Comparison of the present free vibration analysis with Ref. results for a FG cylinder made of Stainless Steel (SS) and Nickel (N) has been made in Table 2[1]. Results of the present method in Table 2 are very close to that of Ref. [1]. Again consider a FG cylinder made of Silicon Nitride (SN) (material no. 1) at its outer surface and Stainless Steel (SS) (material no. 2) at its inner surface (SS-SN FG shell). Hereinafter, everywhere otherwise stated, geometrical parameters of the shell are considered to be  $R = L = 1m$  and  $h = 0.002m$ .

**Table 1** Properties of materials <sup>a</sup> [7]

		$E$	$\nu$	$\rho$
		(Pa)		(kg/m <sup>3</sup> )
Stainless Steel (SS)	$P_0$	$201.04 \times 10^9$	0.3262	8166
	$P_{-1}$	0	0	0
	$P_1$	$3.079 \times 10^{-4}$	$-2.002 \times 10^{-4}$	0
	$P_2$	$-6.534 \times 10^{-7}$	$3.797 \times 10^{-7}$	0
	$P_3$	0	0	0
Silicon Nitride (SN)	$P_0$	$348.43 \times 10^9$	0.24	2370
	$P_{-1}$	0	0	0
	$P_1$	$-3.070 \times 10^{-4}$	0	0
	$P_2$	$2.160 \times 10^{-7}$	0	0
	$P_3$	$-8.946 \times 10^{-11}$	0	0
Nickel (N)	$P_0$	$223.95 \times 10^9$	0.31	8900
	$P_{-1}$	0	0	0
	$P_1$	$-2.794 \times 10^{-4}$	0	0
	$P_2$	$-3.998 \times 10^{-9}$	0	0
	$P_3$	0	0	0

<sup>a</sup>The properties were evaluated at  $T=300$  °K

**Table 2** Comparison of natural frequencies (Hz) for different values of power law exponent ( $N$ ) for simply supported SS-N FG cylindrical shell

circumferential wave number	$N=1$		$N=30$	
	Ref.[1]	Present	Ref.[1]	Present
1	13.211	13.2111	13.526	13.5256
2	4.4742	4.4759	4.5836	4.5830
3	4.1486	4.1496	4.2536	4.2511
4	7.0330	7.0326	7.2085	7.2056
5	11.238	11.2367	11.516	11.5134
6	16.453	16.4520	16.859	16.8571
7	22.633	22.6331	23.192	23.1905
8	29.770	29.7707	30.505	30.5039
9	37.861	37.8621	38.795	38.7945
10	46.904	45.9065	48.061	48.0616

( $m = 1, h/R = 0.002, L/R = 20, P=0$ )

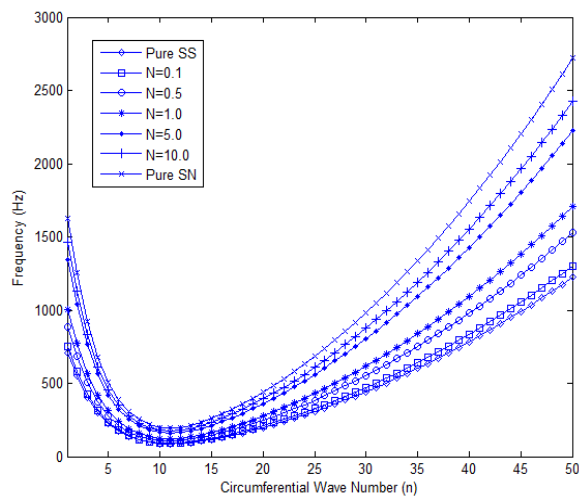


**Fig. 2** Effect of  $N$  on the natural frequencies vs. circumferential wave number ( $n$ );  $m=1, P=0$

The Effect of power law exponent ( $N$ ) on the natural frequencies versus circumferential wave number ( $n$ ) for axial half wave number  $m=1$  is shown in Fig. 2. According to this figure, by increasing the value of  $N$  from zero (pure SS) to infinity (pure SN), all the natural frequencies increase approximately in the same manner (about 2.2~2.3 times). In addition, all frequencies corresponded to FG shells lie between those of pure SS and pure SN shells.

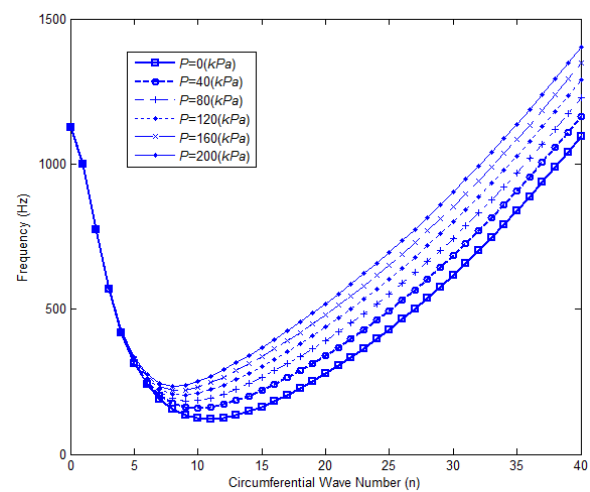


**Fig. 3** Effect of  $P$  on the natural frequencies vs. circumferential wave number ( $n$ );  $m=1, N=1$

It is to be noted that when  $P=0$ , the value of  $N$  do not affect  $n$  corresponded to the fundamental frequency. The effect of internal pressure on the natural frequencies of the shell considered in Fig. 2, for  $m=1$  and  $N=1$ , is shown in Fig. 3. As can be seen from this figure, by increasing the value of  $P$ , the natural frequencies far away from  $n=0$  increase considerably, but the natural frequencies corresponded to  $n < 5$  remain almost unchanged.

This phenomenon is due to the fact that by applying internal pressure, the amount of strain energy required for free vibrations at higher values of circumferential wave numbers, increases. Furthermore, it is to be noted that the  $n$  related to  $\omega_f$  becomes smaller by increasing  $P$ . Also, by increasing  $P$ , the value of  $\omega_f$  is increased about 1.95 times. Fig. 4 shows the variation of  $\omega_f$  versus  $P$  for different values of  $N$ . As can be seen from this figure, by increasing the value of  $P$  for pure SS shell,  $\omega_f$  is increased by 54.5% and for pure SN shell,  $\omega_f$  is increased by 71.3%. For the values of  $0 < N < \infty$ ,  $\omega_f$  is increased between 54.5% to 71.3%.

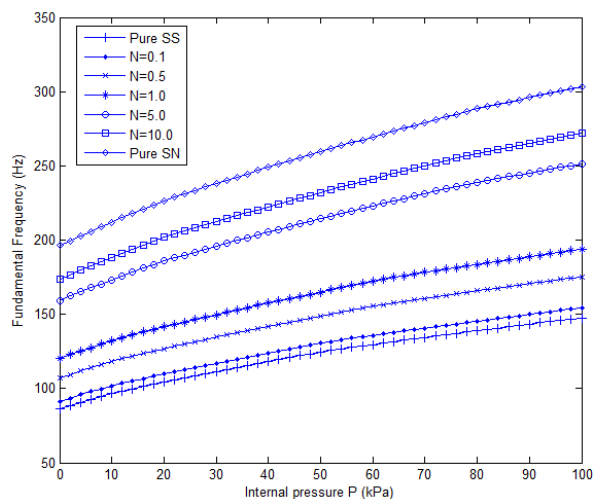


Fig. 4 Effect of  $N$  on  $\omega_f$  vs.  $P$

In Fig. 5, the effect of  $N$  on percentage increase of  $\omega_f$  regarding FG shells in comparison with  $\omega_f$  with respect to pure SS shell is studied by increasing the amount of  $P$ .

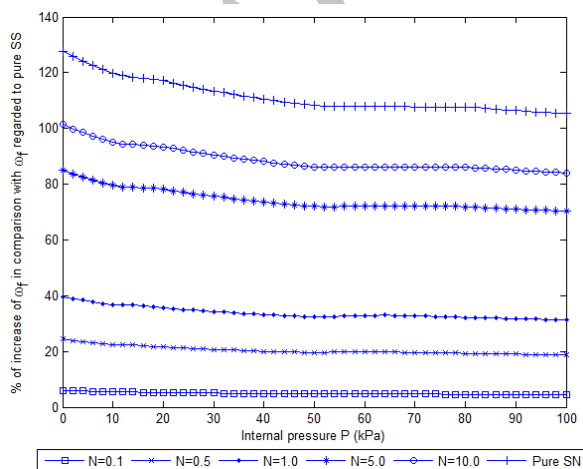


Fig. 5 Percentage increase of  $\omega_f$  for FG shells in comparison with  $\omega_f$  for pure SS shell vs.  $P$

As can be seen from this figure, there is a decreasing trend by increasing  $P$  from  $P = 0(kPa)$  to  $P = 100(kPa)$ . In the case of FG shell ( $N=0.1$ ), the decrement is 1.6% and in the case of pure SS shell, the decrement is 22.3%. For the values of  $N$  ( $0.1 < N < \infty$ ), the decrements lie between 1.6% and 22.3%. Fig. 6 depicts simultaneously percentage increase of  $\omega_f$  regarding FG shell ( $N=0.1$ ) in comparison to  $\omega_f$  with respect to pure SS shell (right axis) as well as the circumferential wave number  $n$  (left axis) by increasing  $P$ .

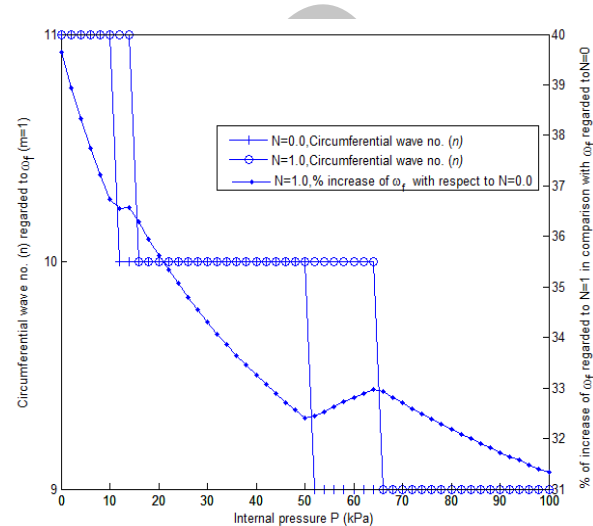


Fig. 6 Percentage increase of  $\omega_f$  for FG shell ( $N=0.1$ ) in comparison to  $\omega_f$  for pure SS shell as well as the corresponding values of  $n$

According to this figure, as the value of  $P$  increases, there is a decreasing trend in percentage increase of  $\omega_f$  regarding to FG shell in comparison to  $\omega_f$  with respect to pure SS shell. But, the opposite trend occurred within the specific ranges of  $P$  in which  $n$  corresponded to the fundamental mode shape differs for  $N=0$  and  $N=0.1$  (i.e.  $P = 12 \sim 16(kPa)$  and  $P = 52 \sim 66(kPa)$ ). By increasing the internal pressure, alteration in the fundamental mode shape number occurred at the beginning and the end of the mentioned ranges for pure SS ( $N=0.0$ ) shell and FG shell ( $N=0.1$ ), respectively. Indeed, increasing the value of  $P$  within the mentioned ranges has less effect on the shell with greater overall stiffness (i.e. FG shell  $N=0.1$ ).

In addition, a similar trend shown in Fig. 6 was observed for values of  $N$  greater than 0.1. Variation of  $\omega_f$  versus  $N$  for different values of  $P$  is illustrated in Fig. 7 for two FGM configurations (i.e. SS-SN and SN-SS). As can be seen from this figure, at  $N=1.0$ , the

values of  $\omega_f$  regarding SS-SN shells are almost equal to the values of  $\omega_f$  corresponding to SN-SS shells.

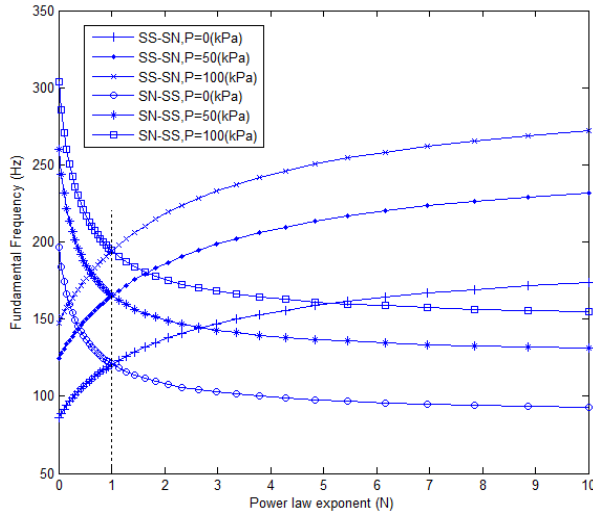


Fig. 7 Variation of  $\omega_f$  vs.  $N$  for different values of  $P$

Also, the slopes of  $\omega_f$ - $N$  graph regarding SS-SN shells are almost equal to the slopes of  $\omega_f$ - $N$  graph corresponding to SN-SS shells. The validity of this interesting result was further investigated within the geometrical ranges  $h/R = 0.002 \sim 0.01$  as well as  $L/R = 1 \sim 10$ . As expected, by increasing the value of  $N$ ,  $\omega_f$  related to SS-SN shell is increased. In contrast, by increasing the value of  $N$ ,  $\omega_f$  with regard to SN-SS shell is decreased. In both cases, by increasing  $P$ ,  $\omega_f$  is increased. Fig. 8 shows the variation of  $\omega_f$  versus  $h/R$  for different values of  $P$  and  $N$ .

As can be observed in this figure, by increasing the value of  $P$  from  $P = 0(kPa)$  to  $P = 100(kPa)$ , for  $N=0.0$ ,  $\omega_f$  is increased to 71.3% at  $h/R=0.002$  and 2.1% at  $h/R=0.01$ . Also, for  $N=1.0$ ,  $\omega_f$  is increased to 61.1% at  $h/R=0.002$  and 1.7% at  $h/R=0.01$ . This percentage increments in  $\omega_f$  reveals that the internal pressure has more effect on  $\omega_f$  at lower values of  $h/R$  and this effect is more at lower values of  $N$ . Fig. 9 shows the variation of  $\omega_f$  versus  $L/R$  for different values of  $P$  and  $N$ . As can be observed in this figure, by increasing the value of  $P$  from  $P = 0(kPa)$  to  $P = 100(kPa)$ , for  $N=0.0$ ,  $\omega_f$  is increased to 71.3% at  $L/R=1$  and 251.8% at  $L/R=10$ . Also, for  $N=1.0$ ,  $\omega_f$  is increased to 61.1% at  $L/R=1$  and 227.0% at  $L/R=10$ . This percentage increments in  $\omega_f$  reveals that the internal pressure has more effect on  $\omega_f$  at higher values

of  $L/R$  and this effect is more significant at lower values of  $N$ .

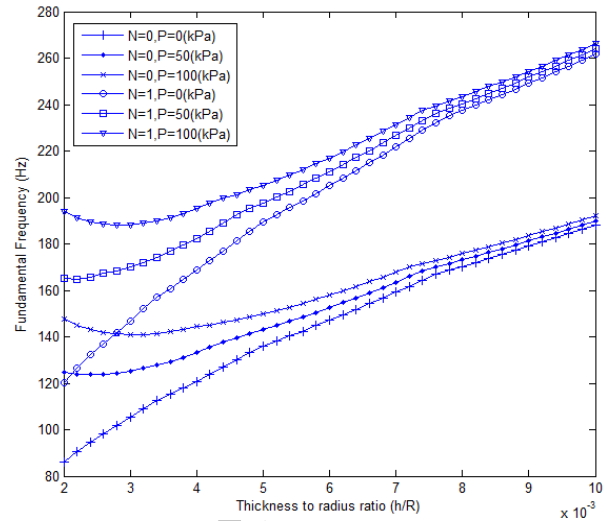


Fig. 8 Variation of  $\omega_f$  vs.  $h/R$  for different values of  $P$  and  $N$

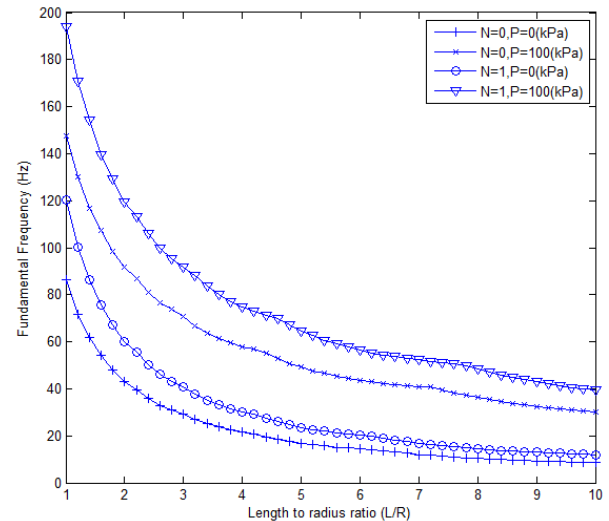


Fig. 9 Variation of  $\omega_f$  vs.  $L/R$  for different values of  $P$  and  $N$

In Fig. 10, variations of  $\omega_f$  as well as  $I_1$  (mass per unit area) versus  $N$  are plotted simultaneously. As depicted in this figure, by increasing the value of  $N$ ,  $\omega_f$  increases, in contrast,  $I_1$  decreases. Since the overall stiffness of the FG shell is increased by increasing  $N$ , beside the decreasing trend of mass, justify the increasing trend in  $\omega_f$  versus  $N$ . The effect of  $N$  on the bending vibration relative to amplitudes in radial direction regarded to  $\omega_f$  are investigated in Fig. 11. As shown in this figure, the relative amplitude regarded to pure SN shell is about 1.85 times greater than that for



pure SS shell. So  $N$  has a considerable effect on the amplitudes of free vibrations. The effect of  $P$  on the bending vibration relative to amplitudes in radial direction regarded to  $\omega_f$  are investigated in Fig. 12. As shown in this figure, the relative amplitude almost is not affected by variation of  $P$ . So the effect of  $P$  on the amplitudes of free vibrations is unimportant.

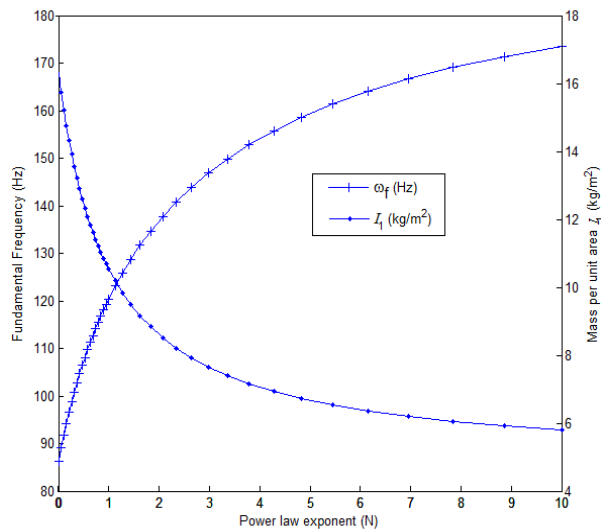


Fig. 10 Variations of  $\omega_f$  as well as  $I_1$  vs.  $N$  ( $P=0$ )

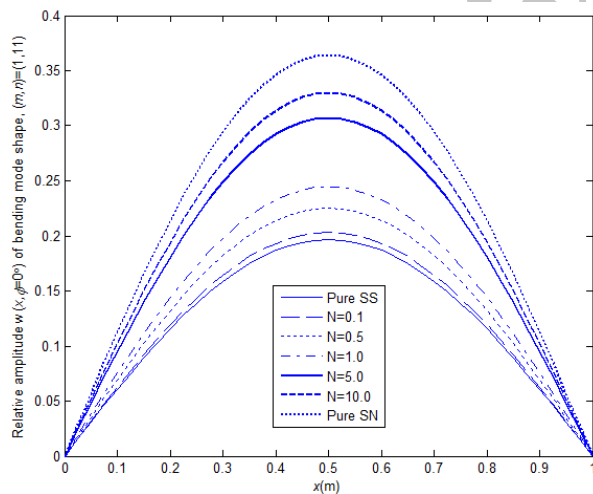


Fig. 11 Effect of  $N$  on the bending vibration relative amplitudes in radial direction ( $P=0$ )

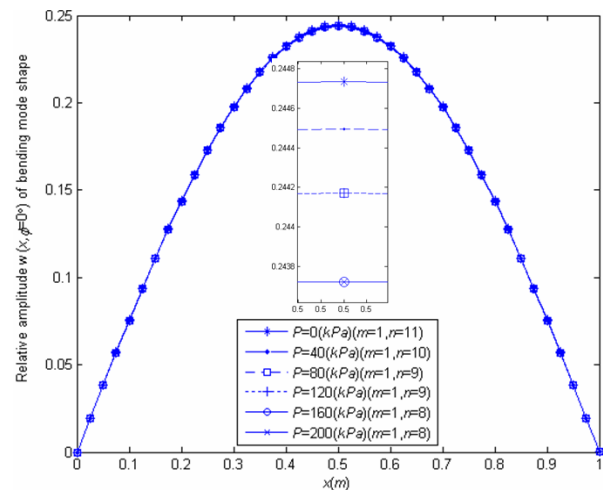


Fig. 12 Effect of  $P$  on the bending vibration relative amplitudes in radial direction ( $N=1.0$ )

## 6 CONCLUSION

A study on the free vibrations of internally pressurized functionally graded (FG) circular cylindrical shells composed of Stainless Steel (SS) and Silicon Nitride (SN) with two different configurations, SS-SN as well as SN-SS, has been presented. The analysis was carried out using First order Shear Deformation Theory (FSDT) based on Love's first approximation theory. A validation of the analysis was achieved by comparing results with those available in the literature.

The study shows that the natural frequencies for all values of  $N$  lie between those of pure SS and pure SN cylindrical shells. Increasing the value of  $P$ , causes the natural frequencies far away from  $n=0$  to increase. In addition, the internal pressure has more effect on fundamental frequency ( $\omega_f$ ) at higher values of  $L/R$ , in contrast, it has more effect on  $\omega_f$  at lower values of  $h/R$ . In both cases, this effect is more significant at lower values of  $N$ . The analysis indicates that fundamental frequency mode number could be affected by both  $N$  and  $P$ . Finally, the values of  $\omega_f$  regarding SS-SN shells are almost equal to the values of  $\omega_f$  corresponding to SN-SS shells. Also, the slopes of  $\omega_f-N$  graph related to SS-SN shells are almost equal to the slopes of  $\omega_f-N$  graph corresponding to SN-SS shells.

## 7 APPENDIX

Differential operators  $L_{ij}$  are as follows:

$$L_{11} = (A_{11}R)_{,xx} + (2A_{16})_{,x\varphi} + \left(\frac{A_{66}}{R} + P\right)_{,\varphi\varphi} - (I_1R)_{,tt}$$

$$L_{12} = L_{21} = (A_{16}R)_{,xx} + (A_{12} + A_{66})_{,x\phi} + \left(\frac{A_{26}}{R}\right)_{,\phi\phi}$$

$$L_{13} = -L_{31} = (A_{12} + RP)_{,x} + \left(\frac{A_{26}}{R}\right)_{,\phi}$$

$$L_{14} = L_{41} = (B_{11}R)_{,xx} + (2B_{16})_{,x\phi} + \left(\frac{B_{66}}{R}\right)_{,\phi\phi} - (I_2R)_{,tt}$$

$$L_{15} = L_{51} = (B_{16}R)_{,xx} + (B_{12} + B_{66})_{,x\phi} + \left(\frac{B_{26}}{R}\right)_{,\phi\phi}$$

$$L_{22} = (A_{66}R)_{,xx} + (2A_{26})_{,x\phi} + \left(\frac{A_{22}}{R} + P\right)_{,\phi\phi} - \frac{H_{44}}{R} - (I_1R + 2I_2)_{,tt}$$

$$L_{23} = -L_{32} = (A_{26} + H_{45})_{,x} + \left(\frac{A_{22}}{R} + \frac{H_{44}}{R} + RP\right)_{,\phi}$$

$$L_{24} = L_{42} = (B_{16}R)_{,xx} + (B_{12} + B_{66})_{,x\phi} + \left(\frac{B_{26}}{R}\right)_{,\phi\phi} + H_{45}$$

$$L_{25} = L_{52} = (B_{66}R)_{,xx} + (2B_{26})_{,x\phi} + \left(\frac{B_{22}}{R}\right)_{,\phi\phi} + H_{44} - (I_2R + I_3)_{,tt}$$

$$L_{33} = (H_{55}R)_{,xx} + (2H_{45})_{,x\phi} + \left(\frac{H_{44}}{R} + P\right)_{,\phi\phi} - \frac{A_{22}}{R} - (I_1R)_{,tt}$$

$$L_{34} = L_{43} = (H_{55}R - B_{12})_{,x} + \left(H_{45} - \frac{B_{26}}{R}\right)_{,\phi}$$

$$L_{35} = -L_{53} = (H_{45}R - B_{26})_{,x} + \left(H_{44} - \frac{B_{22}}{R}\right)_{,\phi}$$

$$L_{44} = (D_{11}R)_{,xx} + (2D_{16})_{,x\phi} + \left(\frac{D_{66}}{R}\right)_{,\phi\phi} - H_{55}R - (I_3R)_{,tt}$$

$$L_{45} = L_{54} = (D_{16}R)_{,xx} + (D_{12} + D_{66})_{,x\phi} + \left(\frac{D_{26}}{R}\right)_{,\phi\phi} - H_{45}R$$

$$L_{55} = (D_{66}R)_{,xx} + (2D_{26})_{,x\phi} + \left(\frac{D_{22}}{R}\right)_{,\phi\phi} - H_{44}R - (I_3R)_{,tt}$$

## REFERENCES

- [1] Loy, C. T., Lam, K. Y., and Reddy, J. N., "Vibration of functionally graded cylindrical shells", International Journal of Mechanical Sciences, Vol. 41, 1999, pp. 309-324.
- [2] Pradhan, S. C., Loy, C. T., Lam, K. Y., and Reddy J. N., "Vibration characteristics of functionally graded cylindrical shells under various boundary condition", Applied Acoustics, Vol. 61, 2000, pp. 111-129.
- [3] Ng, T. Y., Lam, K. Y., Liew, K. M., and Reddy, J. N., "Dynamic stability analysis of functionally graded cylindrical shells under periodic axial loading", Int. J. of Solids and Structures, Vol. 38, 2001, pp. 1295-1309.
- [4] Liew, K. M., Yang, J., and Wu, Y. F., "Nonlinear vibration of a coating-FGM-substrate cylindrical panel subjected to a temperature gradient", Comput. Methods Appl. Mech. Engrg, Vol. 195, 2006, pp. 1007-1026.
- [5] Darabi, M., Darvizeh, M., and Darvizeh, A., "Non-linear analysis of dynamic stability for functionally graded cylindrical shells under periodic axial loading", Composite Structures, Vol. 83, No. 2, 2008, pp. 201-211.
- [6] Ansari, R., and Darvizeh, M., "Prediction of dynamic behaviour of FGM shells under arbitrary boundary conditions", Composite Structures, Vol. 85, No. 4, 2008, pp. 284-292.
- [7] Haddadpour, H., Mahmoudkhani, S., and Navazi, H. M., "Free vibration analysis of functionally graded cylindrical shells including thermal effects", Thin-Walled Structures, Vol. 45, 2007, pp. 591-599.
- [8] Khalili, S. M. R., Malekzadeh, M., and Davar, A., "Dynamic response of functionally graded circular cylindrical shells", Advanced Materials Research, Vol. 47-50, 2008, pp. 608-611.
- [9] Khalili, S. M. R., Azarafza, R., and Davar, A., "Transient dynamic response of initially stressed composite circular cylindrical shells under radial impulse load", Composite Structures, Vol. 89, No. 2, 2009, pp. 275-284.